

A Quantum Otto Engine with Shortcuts to Thermalization and Adiabaticity

A. Pedram,^{1,*} S. C. Kadioğlu,^{1,†} A. Kabakçıoğlu,^{1,‡} and Ö. E. Müstecaplıoğlu^{1,2,§}

¹*Department of Physics, Koç University, Istanbul, Sarıyer 34450, Türkiye*

²*TÜBİTAK Research Institute for Fundamental Sciences, 41470 Gebze, Türkiye*

We investigate the energetic advantage of accelerating a quantum harmonic oscillator Otto engine by use of shortcuts to adiabaticity (for the power and compression strokes) and to equilibrium (for the hot isochore), by means of counter-diabatic (CD) driving. By comparing various protocols with and without CD driving, we find that, applying both type of shortcuts leads to enhanced power and efficiency even after the driving costs are taken into account. The hybrid protocol not only retains its advantage in the limit cycle, but also recovers engine functionality (i.e., a positive power output) in parameter regimes where an uncontrolled, finite-time Otto cycle fails. We show that controlling three strokes of the cycle leads to an overall improvement of the performance metrics compared with controlling only the two adiabatic strokes. Moreover, we numerically calculate the limit cycle behavior of the engine and show that the engines with accelerated isochoric and adiabatic strokes display a superior power output in this mode of operation.

Keywords: open quantum systems; quantum thermodynamics; quantum heat engines;

I. INTRODUCTION

Enhancing the performance of heat engines has been a long-standing objective in the field of thermodynamic cycle investigations. The pinnacle of these endeavors is reflected in Carnot's second law of thermodynamics, which establishes an upper limit on the efficiency of heat engines [1]. This limit can, in principle, be attained through a Carnot cycle, comprising reversible processes. However, while the Carnot engine achieves this limit, it is unable to generate any power due to the quasi-static nature of its processes. Practical heat engine cycles such as Otto, Diesel, or Stirling face the challenge of balancing efficiency and power, necessitating real-world engines to complete a cycle within a finite time, albeit with lower efficiency. Of particular significance is the efficiency at maximum power, which was studied by Curzon and Ahlborn in their seminal paper [2].

Currently, there is ongoing research in quantum heat engines and refrigerators [3–7]. Since the pioneering work by Scovil and Schulz-DuBois [8], quantum heat engines have been extensively studied theoretically [9–36], and successful experimental demonstrations have been recently reported [37–44]. Despite these theoretical and experimental developments, it is still an open question whether the quantum advantage can lead to Carnot efficiency or better at finite power [45–47]. It is, therefore, crucial to study the potential and limitations of quantum thermal devices and investigate methods to boost their finite-time performance.

A specific type of control techniques which are collec-

tively known as shortcuts to adiabaticity (STA) have gained a particular interest in the study of quantum heat engines. The central idea in STA is to design protocols to drive the system by emulating its adiabatic dynamics in finite time [48, 49]. Since its foundation [50–53] different approaches have been developed to engineer STA, such as using dynamical invariants, [53, 54], inversion of scaling laws [55, 56] and the fast-forward technique [57–59]. In recent years, successful experimental realizations of STA has been reported in the literature [60–63].

STA has been extensively explored as a means to enhance the performance of quantum refrigerators [64, 65] and boost the power output of quantum harmonic oscillator [66–69] and spin chain [70–72] based quantum heat engines by emulating adiabatic strokes within finite time frames. Previous studies in these domains have commonly assumed a rapid thermalization step. However, with the growing interest in the application of STA to open quantum systems, recent research has increasingly focused on the possibility of achieving swift thermalization using various techniques [73–80]. These approaches are often referred to as fast thermalization, shortcuts to thermalization (STT) or shortcuts to equilibrium (STE). Since quantum heat engines contain thermalization branches, study of these techniques is of paramount importance in order to optimize the power and efficiency of these devices [75, 78–80].

Motivated by these advancements, we conduct an analysis of the energy dynamics, power output, and efficiency characteristics of an Otto cycle utilizing a quantum harmonic oscillator as its working medium within a finite time frame. To achieve this, we employ shortcuts to adiabaticity (STA) during the expansion and compression strokes, while implementing shortcuts to equilibrium (STE) during the hot isochoric stroke, resulting in what we refer to as an STÆ engine. In our investigation, we compare the thermodynamic

* apedram19@ku.edu.tr

† skadioglu16@ku.edu.tr

‡ akabakcioglu@ku.edu.tr

§ omustecap@ku.edu.tr

performance metrics of this engine with an uncontrolled non-adiabatic quantum Otto (UNA engine) and a quantum Otto engine in which only the adiabatic strokes are accelerated using CD-driving (STA engine).

For a comprehensive evaluation of the thermodynamic performance within controlled dynamics, it is essential to meticulously account for the energetic expenses associated with implementing the control protocols [67, 68, 70, 71]. In this regard, we adopt a widely employed cost measure to quantify the energetic requirements of the shortcuts to adiabaticity (STA) protocol during the adiabatic strokes. Additionally, we introduce a novel cost measure based on the dissipative work performed by the environment [81] specifically for the shortcuts to equilibrium (STE) protocol. This dual approach enables a thorough assessment of the energetic aspects involved in implementing both STA and STE protocols.

Initially, we conduct a thermodynamic analysis of the three engines (UNA, STA, and ST \ddot{A}) by considering a single cycle following the preparation phase. Subsequently, we extend our examination to their respective limit cycles. Our findings clearly demonstrate that the ST \ddot{A} engine, incorporating both shortcuts to adiabaticity (STA) and shortcuts to equilibrium (STE) protocols, attains superior power output and efficiency when compared to the STA-only engine and the UNA engine.

This manuscript is organised as follows. In Sec. II we briefly introduce the quantum Otto cycle. In Sec. III the scheme for STA using counterdiabatic driving is introduced. In Sec. IV the protocol for the fast driving of the otto cycle towards thermalization is introduced. In Sec. V we describe the quantum Otto engine for which both STA and STE is used. In Sec. VI we present our results and finally in Sec. VII we draw our conclusions.

II. QUANTUM HARMONIC OTTO CYCLE

We study a finite-time quantum Otto cycle and consider the working medium to be harmonic oscillator with a time dependent frequency. The Hamiltonian for harmonic oscillator is

$$\hat{H}_0 = \hat{p}^2/2m + m\omega_t^2\hat{x}^2/2 \quad (1)$$

in which \hat{x} and \hat{p} are the position and momentum operators respectively and ω_t is the time dependent frequency and m is the mass of the oscillator. As shown in Fig. 1, the cycle consists of the following strokes.

- (1) Adiabatic compression (1 \rightarrow 2): Unitary evolution for a duration of τ_{12} while the frequency increases from ω_c to ω_h .

- (2) Hot isochore (2 \rightarrow 3): Heat transfer from the hot bath to the system for a duration of τ_{23} as the system equilibrates with the bath at temperature T_h at fixed frequency.
- (3) Adiabatic expansion (3 \rightarrow 4): Unitary evolution for a duration of τ_{34} while the frequency decreases from ω_h to ω_c .
- (4) Cold isochore (4 \rightarrow 1): Heat transfer from the system to the cold bath for a duration of τ_{41} as the system equilibrates with the bath at temperature T_c at fixed frequency.

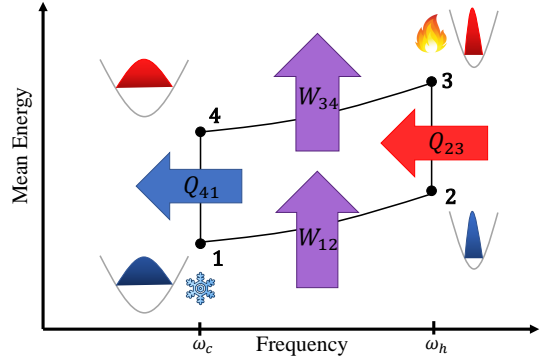


FIG. 1. Schematic representation of a quantum Otto cycle.

During the adiabatic steps the system is decoupled from the heat baths, and the frequency is varied over time, at a rate bounded by the adiabatic theorem [52], so that the populations of the drifting energy levels remain unchanged. The resulting isentropic evolution is more restrictive than the classical adiabaticity condition of constant entropy.

Mathematical formulations of the adiabatic time evolution for an isolated quantum system employ a time-scale separation between fast and slow degrees of freedom, yielding product states as solutions. For the compression and expansion strokes of the QHO Otto engine, this condition implies that the system will always remain in an instantaneous eigenstate of the time-dependent Hamiltonian. The unitary time evolution of such a process, which ideally takes infinite time, can be solved exactly and has zero entropy production. The average work and heat exchange values during the cycle is given by [82, 83],

$$\langle W_{12} \rangle = \frac{\hbar}{2}(\omega_h Q_{12}^* - \omega_c) \coth\left(\frac{\beta_c \hbar \omega_c}{2}\right) \quad (2)$$

$$\langle Q_{23} \rangle = \frac{\hbar \omega_h}{2} \left[\coth\left(\frac{\beta_h \hbar \omega_h}{2}\right) - Q_{12}^* \coth\left(\frac{\beta_c \hbar \omega_c}{2}\right) \right] \quad (3)$$

$$\langle W_{34} \rangle = \frac{\hbar}{2}(\omega_c Q_{34}^* - \omega_h) \coth\left(\frac{\beta_h \hbar \omega_h}{2}\right) \quad (4)$$

$$\langle Q_{41} \rangle = \frac{\hbar \omega_c}{2} \left[\coth\left(\frac{\beta_c \hbar \omega_c}{2}\right) - Q_{34}^* \coth\left(\frac{\beta_h \hbar \omega_h}{2}\right) \right] \quad (5)$$

where W refers to the work input and Q refers to the heat input to the engine during the indicated strokes.

β_c and β_h are the inverse temperatures for the cold and hot bath respectively. The terms Q_{12}^* and Q_{34}^* are the adiabaticity parameters and their values depend on the driving scheme [67]. We are employing a sign convention in which all the incoming fluxes (heat and work) are taken to be positive [35, 84].

In order to study the finite-time Otto cycle, we need to consider the time evolution along each stroke separately. The unitary evolution of the adiabatic strokes is governed by

$$\partial_t \hat{\rho} = -\frac{i}{\hbar} [\hat{H}_0, \hat{\rho}], \quad (6)$$

where $\hat{\rho}$ is the system's density matrix. For the duration of the isochoric strokes, a Markovian open system dynamics given by a Gorini–Kossakowski–Sudarshan–Lindblad (GKLS) master equation governs the system's dynamics,

$$\partial_t \hat{\rho} = -\frac{i}{\hbar} [\hat{H}_0, \hat{\rho}] + \mathcal{D}(\hat{\rho}), \quad (7)$$

in which $\mathcal{D}(\hat{\rho})$ is the dissipation superoperator which must conform to Lindblad's form for a Markovian evolution

$$\mathcal{D}(\hat{\rho}) = k_{\uparrow}(\hat{a}^\dagger \hat{\rho} \hat{a} - \frac{1}{2}\{\hat{a}\hat{a}^\dagger, \hat{\rho}\}) + k_{\downarrow}(\hat{a}\hat{\rho}\hat{a}^\dagger - \frac{1}{2}\{\hat{a}^\dagger\hat{a}, \hat{\rho}\}). \quad (8)$$

The k_{\uparrow} and k_{\downarrow} are called heat conductance rates and the heat conductivity (heat transport rate) defined as $\Gamma \equiv k_{\downarrow} - k_{\uparrow}$ [4]. Note that, heat transport is not the only source of irreversibility in a quantum heat engine. Non-commutativity of the Hamiltonians at different times results in an additional dissipation channel, dubbed "quantum friction" citePhysRevE.65.055102.

In some of the research works on the cycle analysis of the quantum heat engines it is commonly assumed that the thermalization times are much shorter than the compression and expansion times, therefore the thermalization times are neglected. [45, 67–70]. However, this assumption requires heat transport rates to be large, a circumstance for which it is shown that the optimal power production happens when the cycle times are vanishingly small [4, 13, 21].

Another line of reasoning to justify small thermalization times incisochoric process is that, for the frequency to stay constant (hence, the Hamiltonian to be static), the duration of the system-bath interaction must be shorter than the duration of the isentropic process. However, assuming that there exists a considerable energy exchange between the system and the bath or that the system equilibrates to the temperature of the bath, controlling the interaction time is equivalent to adjusting the system-bath coupling. However, a large system-bath coupling also implies a large heat transport rate. Additionally, in a thermalization map, which follows a GKLS

type master equation, there is an implicit assumption that the thermalization time (which scales proportional to the inverse of the system-bath interaction energy), is longer than the relaxation dynamics of the bath and the unperturbed dynamics of the system [9]. Therefore, for a realistic and consistent thermodynamic analysis of a quantum heat engine in its full generality, it is important to take into account the effect of thermalization times without imposing additional assumptions.

In order to see the effect of the duration of isochoric strokes, we take the total cycle time to be $\tau_{tot} = \tau_{12} + \tau_{23} + \tau_{34} + \tau_{41}$. We assume that $\tau_{adi} = \tau_{12} = \tau_{34}$ and $\tau_{iso} = \tau_{23} = \tau_{41}$. The engine power can be expressed as,

$$P = -\frac{\langle W_{12} \rangle + \langle W_{34} \rangle}{\tau_{tot}} \quad (9)$$

in which $\tau_{tot} = 2\tau_{adi} + 2\tau_{iso}$. For an ideal engine, efficiency becomes

$$\eta = -\frac{\langle W_{12} \rangle + \langle W_{34} \rangle}{\langle Q_{23} \rangle}. \quad (10)$$

Due to the fact that the ideal adiabatic and isochoric strokes are quasi-static, upon implementing a full cycle in finite time, the state the working medium of the engine doesn't precisely return to the initial state from which the cycle started. Therefore, for a complete study of a finite time quantum heat engine a limit cycle analysis has to be taken into account and the thermodynamic behavior of the engine in this mode of operation needs to be addressed [4, 19, 32]. A general quantum process is described by a completely positive trace preserving (CPTP) map. The quantum channel for the entire cycle is a composition of four CPTP maps,

$$\varepsilon(\hat{\rho}) = \varepsilon_{4 \rightarrow 1} \circ \varepsilon_{3 \rightarrow 4} \circ \varepsilon_{2 \rightarrow 3} \circ \varepsilon_{1 \rightarrow 2}(\hat{\rho}) \quad (11)$$

which makes itself CPTP. Due to the Brouwer fixed-point theorem, every such channel should have at least one density operator fixed point ρ^* such that [85]

$$\varepsilon(\hat{\rho}^*) = \hat{\rho}^*. \quad (12)$$

Lindblad showed that relative entropy (KL-divergence) between a state and a reference state is contractive under CPTP maps [86]. Later, Petz proved that a variety of metrics (including the Bures metric) are monotone (contractive) under CPTP maps [87]. These theorems can be expressed mathematically as

$$D_{KL}(\varepsilon(\hat{\rho}) || \varepsilon(\hat{\rho}_{ref})) \leq D_{KL}(\hat{\rho} || \hat{\rho}_{ref}), \quad (13)$$

$$D(\varepsilon(\hat{\rho}), \varepsilon(\hat{\rho}_{ref})) \leq D(\hat{\rho}, \hat{\rho}_{ref}) \quad (14)$$

Here, D_{KL} is the relative entropy (which is not a metric but a divergence function) and D is a metric on the statistical manifold of the density operators. According to these theorems, the two states become less and less distinguishable upon successive application of the map

ε . If the fixed point of the CPTP map is unique, the density operator will monotonically approach the steady-state via the dynamical map [88]. In this case, if we take $\hat{\rho}_{\text{ref}} = \hat{\rho}^*$, Eq. (12) and Sec. II imply that upon successive application of the quantum channel, the system monotonically approaches the fixed point.

III. STA BY CD-DRIVING

In $1 \rightarrow 2$ and $3 \rightarrow 4$ the quantum system is isolated and work is performed by changing the frequency between ω_c and ω_h , which are fixed as design parameters. We now consider a counter-diabatic drive on the system by means of a control Hamiltonian added to \hat{H}_0 , i.e.,

$$\hat{H}_{CD}(t) = \hat{H}_0(t) + \hat{H}_1(t) \quad (15)$$

such that the resulting dynamics given by

$$\partial_t \hat{\rho} = -\frac{i}{\hbar} [\hat{H}_{CD}, \hat{\rho}] \quad (16)$$

is identical to the approximate adiabatic evolution under \hat{H}_0 alone. For a closed system, the general form of \hat{H}_1 reads [52]

$$\hat{H}_1(t) = i\hbar \sum_n (|\partial_t n\rangle\langle n| - \langle n|\partial_t n\rangle|n\rangle\langle n|) \quad (17)$$

where $|n\rangle$ is the n -th eigenstate of $\hat{H}_0(t)$. This STA protocol requires that $\langle \hat{H}_1(0) \rangle = \langle \hat{H}_1(\tau) \rangle = 0$. Hence, the frequency satisfies the following initial and final conditions.

$$\begin{aligned} \omega_t(0) &= \omega_i, & \dot{\omega}_t(0) &= 0, & \ddot{\omega}_t(0) &= 0, \\ \omega_t(\tau) &= \omega_f, & \dot{\omega}_t(\tau) &= 0, & \ddot{\omega}_t(\tau) &= 0. \end{aligned} \quad (18)$$

An interpolating ansatz which satisfies the mentioned boundary conditions is [89],

$$\omega_t = \omega_i + (\omega_f - \omega_i)[10s^3 - 15s^4 + 6s^5] \quad (19)$$

in which $s = t/\tau_{\text{adi}}$. For a time-dependent QHO, \hat{H}_1 in Eq.(17) can be expressed as [90]

$$\hat{H}_1 = -\frac{\dot{\omega}_t}{4\omega_t} (\hat{x}\hat{p} + \hat{p}\hat{x}). \quad (20)$$

The total Hamiltonian governing the time evolution of the STA controlled QHO becomes

$$\hat{H}_{CD} = \frac{\hat{p}^2}{2m} + \frac{m\omega_t^2 \hat{x}^2}{2} - \frac{\dot{\omega}_t}{4\omega_t} (\hat{x}\hat{p} + \hat{p}\hat{x}). \quad (21)$$

Hence, for a time dependent QHO, the total Hamiltonian is quadratic in \hat{x} and \hat{p} and can be considered a generalized QHO [91],

$$\hat{H}_{CD} = \hbar\Omega_t(\hat{b}_t^\dagger \hat{b}_t + 1/2), \quad (22)$$

with an effective frequency Ω_t and the ladder operator \hat{b}_t given by

$$\Omega_t = \omega_t \sqrt{1 - \dot{\omega}_t^2/4\omega_t^4}; \quad (23)$$

$$\hat{b}_t = \sqrt{\frac{m\Omega_t}{2\hbar}} (\zeta_t \hat{x} + \frac{i\hat{p}}{m\Omega_t}). \quad (24)$$

The work done during this process is given by

$$W = \int_0^{\tau_{\text{adi}}} \text{Tr}(\dot{\hat{H}}_0(t)\hat{\rho}(t))dt \quad (25)$$

The expectation value of the CD driving is defined as [67],

$$\begin{aligned} \langle \hat{H}_1(t) \rangle &= \langle \hat{H}_{CD}(t) \rangle - \langle \hat{H}_0(t) \rangle = \\ &\frac{\omega_t}{\omega_i} \langle \hat{H}_0(t) \rangle \left(\frac{\omega_t}{\Omega_t} - 1 \right). \end{aligned} \quad (26)$$

In order to obtain an accurate thermodynamic description of this controlled process, one should also keep track of the energy cost of CD-driving. The energetic cost of CD driving can be given as time average of $\langle \hat{H}_1(t) \rangle$ [67].

$$C_{\text{STA}} = \frac{1}{\tau_{\text{adi}}} \int_0^{\tau_{\text{adi}}} \langle \hat{H}_1(t) \rangle dt. \quad (27)$$

IV. STE BY CD-DRIVING

For open quantum systems, eigenvalues of the density matrix are time dependent. The time evolution of the density matrix can be written in terms of changes in its eigenprojectors and changes in the eigenvalues. Such a trajectory map can be written as

$$\dot{\hat{\rho}} = -\frac{i}{\hbar} [\hat{H}_{CD}, \hat{\rho}] + \sum_n \partial_t \lambda_n(t) |n_t\rangle\langle n_t|. \quad (28)$$

It is known that (after a modification to make it norm preserving) we can cast Eq. (28) into a Lindblad-like form [76],

$$\partial_t \tilde{\rho} = \sum_{mn} \gamma_{mn} (\tilde{L}_{mn} \tilde{\rho} \tilde{L}_{mn}^\dagger - \frac{1}{2} \{ \tilde{L}_{mn}^\dagger \tilde{L}_{mn}, \tilde{\rho} \}), \quad (29)$$

in which \tilde{L}_{mn} and γ_{mn} are the jump operators and the dissipation rates in the Lindblad-like master equation for a unitarily equivalent trajectory $\tilde{\rho}$. In [76] it is shown that, using the CD-driven STE framework, one can achieve the fast thermalization of a time-dependent QHO from an initial to a final thermal state. For an open and time-dependent QHO, we can write the trajectory map for the unitary transformed density matrix $\tilde{\rho} = \hat{U}_x \hat{\rho} \hat{U}_x^\dagger$ with $\hat{U}_x = \exp(im\alpha_t \hat{x}^2/2\hbar)$ as [76],

$$\partial_t \tilde{\rho} = \frac{-i}{\hbar} \left[\frac{\hat{p}^2}{2m} + \frac{1}{2} m\tilde{\omega}_{CD}^2 \hat{x}^2, \tilde{\rho} \right] - \gamma_t [\hat{x}, [\hat{x}, \tilde{\rho}]]. \quad (30)$$

In which $\tilde{\omega}_{CD}$ is the effective frequency and γ_t is the effective dissipation rate. Such a procedure for shortcut to thermalization can be implemented by modulation of the driving frequency and the dephasing strength [76, 77].

For Eq. (30) we have [76],

$$\omega_{CD}^2 = \omega_t^2 - \alpha_t^2 - \dot{\alpha}_t; \quad (31)$$

$$\gamma_t = \frac{m\omega_t}{\hbar} \frac{\dot{u}_t}{(1-u_t)^2}; \quad (32)$$

$$u_t = e^{-\beta_t \hbar \omega_t}; \quad (33)$$

$$\alpha_t = \zeta_t - \dot{\omega}/2\omega_t; \quad (34)$$

$$\zeta_t = -\frac{\dot{\omega}}{2\omega_t} + \frac{\dot{u}_t}{1-u_t^2}. \quad (35)$$

Here, β_t is the inverse temperature at time t . Similar to the STA case, shortcut to equilibrium is achieved for a general setup by requesting ω_t to follow Eq. (19) (with $s = t/\tau_{iso}$) and β_t to conform to the ansatz [76],

$$\beta_t = \beta_i + (\beta_f - \beta_0)[10s^3 - 15s^4 + 6s^5], \quad (36)$$

in which $s = t/\tau_{iso}$. For this protocol, an entropy based definition for the infinitesimal thermal energy and work can be calculated is given in [81].

$$d\mathcal{Q} = dQ - dW_{CD} = \text{Tr} [\tilde{\mathcal{D}}_{CD}(\tilde{\rho}) \dot{\hat{H}}_0] dt; \quad (37)$$

$$d\mathcal{W} = dW + dW_{CD} = \text{Tr} [\tilde{\rho} \dot{\hat{H}}_0 - i [\hat{H}_0, \tilde{H}_{CD}]] dt \quad (38)$$

in which $\tilde{\mathcal{D}}_{CD} = -\gamma_t [\hat{x}, [\hat{x}, \tilde{\rho}]]$ is the transformed dissipator contributing to the incoherent evolution in Eq. (30). $dW_{CD} = -i\text{Tr}[[\hat{H}, \tilde{H}_{CD}]\tilde{\rho}]dt$ is the environment-induced dissipative work, due to the CD evolution along the trajectory. $d\mathcal{Q}$ and $d\mathcal{W}$ are heat and work calculated in the instantaneous eigenbasis of $\tilde{\rho}$. In Eq. (37) and Eq. (38), dQ and dW signify the infinitesimal changes in the conventional definitions of heat $Q = \text{Tr}[\dot{\hat{H}}_0]$ and work $W = \text{Tr}[\dot{\hat{\rho}} \dot{\hat{H}}_0]$, resulting from Spohn separation [92], in which the coherent (dissipative) changes of the internal energy due to the master equation is phenomenologically labelled as work (heat).

However, it is argued in [81] that for a general evolution of an open quantum system, the contribution of changes in the internal energy which one can label as heat must also coincide with the contribution associated with changes in the entropy and in general, Spohn separation doesn't respect this condition. Hence, the contribution to the changes in the internal energy associated with changes in the eigenvalues of the density matrix is called heat and the contribution associated with the changes in the eigenprojectors is called work and for the CD-driven harmonic oscillator driven to thermalization, these contributions take the form given in Eq. (37) and Eq. (38) as discussed in [81]. Therefore, for the driven system described in this section, the actual values for heat (\mathcal{Q}) and work (\mathcal{W}) during the process can be found by integrating Eq. (37) and Eq. (38) throughout the trajectory. Since during an isochoric process the Hamiltonian

is static ($\dot{\hat{H}}_0 = 0$) we can define the integral of dW_{CD} through the trajectory \mathcal{C} during this process as a cost function as,

$$C_{\text{STE}} = \int_{\mathcal{C}} dW_{CD} = -i \int_0^{\tau_{iso}} \text{Tr}[[\hat{H}_0, \tilde{H}_{CD}]\tilde{\rho}]dt. \quad (39)$$

This cost is not defined operationally, and it quantifies the total environment-induced dissipative work throughout the isochoric process. However, any driving protocol must expend at least the amount of energy given in Eq. (39) to drive the system for the duration of the isochore. Therefore this can be thought of as a lower bound on any operational cost that one can define for such a process.

V. OTTO ENGINE WITH CD DRIVEN STA AND STE

Using the frameworks explained in the previous sections, we propose a CD driven Otto engine with a QHO as a working medium. In Fig. 1 we boost the engine using CD driven STA protocols for expansion and compression and using a CD driven STE protocol for the hot isochore. The cold isochore is modeled by a Markovian master equation and no control Hamiltonian is applied during this step.

Adiabatic evolution implies $\beta_f \omega_f = \beta_i \omega_i$. Hence, after an adiabatic driving for the compression (expansion) stroke, the evolution of the system leads to a density matrix whose statistical distance is close to the thermal density matrix at $\omega_2 = \omega_h$ and $T_2 = (\omega_h/\omega_c) \times T_c$ ($\omega_4 = \omega_c$ and $T_4 = (\omega_c/\omega_h) \times T_c$). We can quantify this statistical distance using fidelity. However, due to the non-commutivity of the control and system Hamiltonians, there will be quantum friction which will manifest itself as coherence terms on the final density matrix. Also, due to the fact that for an isochoric process the frequency must be kept constant, we will use $\omega_t = \omega_h$ throughout the CD-driven hot isochoric stroke, which means that in order to achieve STE we will only consider modulation of the dephasing strength.

We distinguish between the thermodynamic efficiency (η^{th}) of the control engine, which doesn't take into account the control costs and is given by an expression similar to Eq. (10), and the operational efficiency (η^{op}) which considers the energetic costs. The operational efficiency for the CD-driven Otto engine can be calculated taking into account the costs for STA and STE protocols.

$$\eta^{op} = -\frac{W_{12} + W_{34}}{\mathcal{Q}_{23} + C_{adi}^{1 \rightarrow 2} + C_{iso}^{2 \rightarrow 3} + C_{adi}^{3 \rightarrow 4}}. \quad (40)$$

In Eq. (40), W_{12} and W_{34} are calculated using Eq. (25) and \mathcal{Q}_{23} is calculated by integrating Eq. (37). $C_{adi}^{1 \rightarrow 2}$, $C_{iso}^{2 \rightarrow 3}$ and $C_{adi}^{3 \rightarrow 4}$ are the driving costs for the compression,

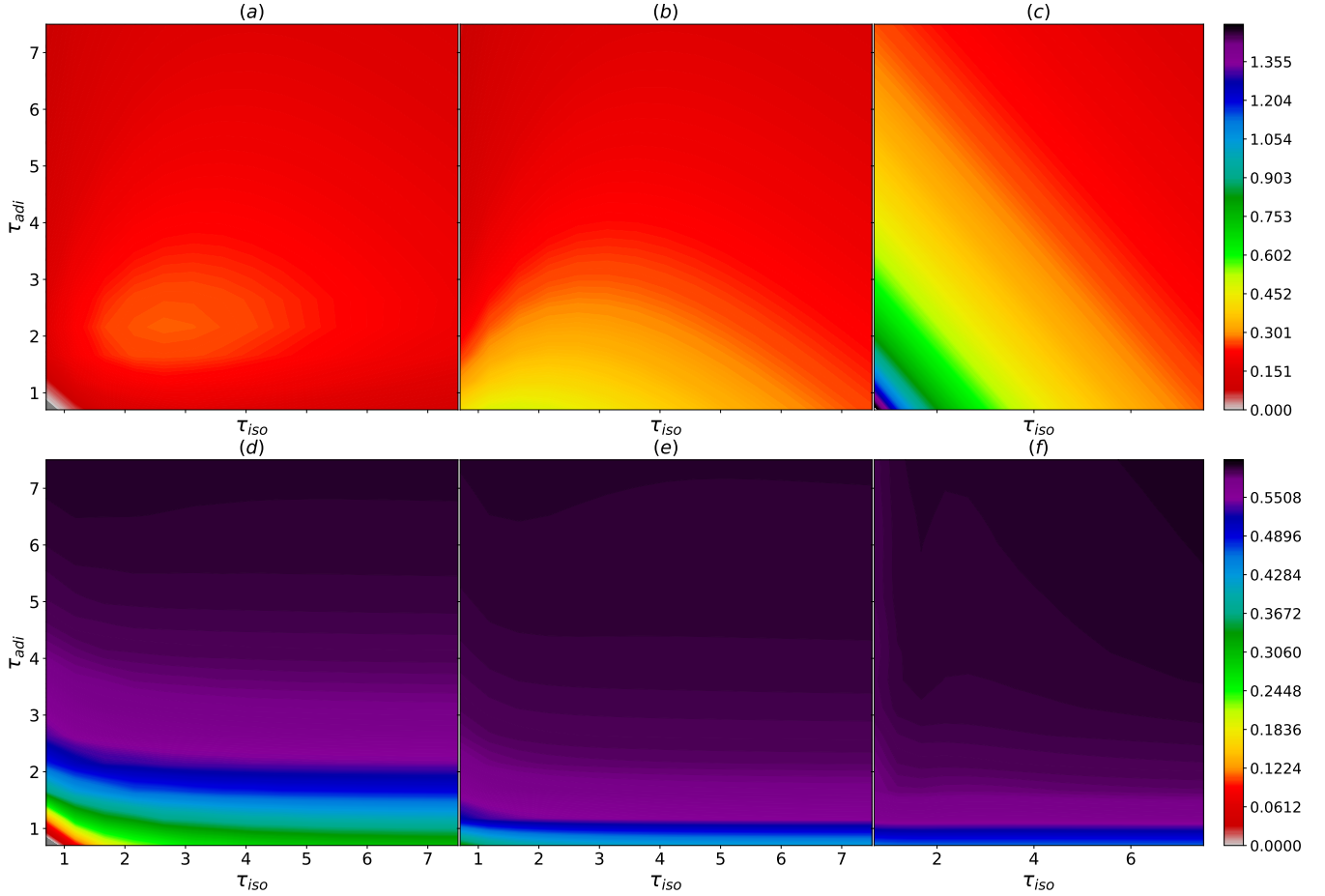


FIG. 2. Power and efficiency of the Otto engine as a function of the duration of the isochoric and adiabatic branches. Top row: Power vs τ_{adi} and τ_{iso} for the (a) UNA engine; (b) STA engine; (c) STÆ engine. Bottom row: Efficiency vs τ_{adi} and τ_{iso} for the (d) UNA engine; (e) STA engine; (f) STÆ engine. Negative power and efficiency results for the finite time Otto engine are greyed out.

cold isochore and expansion strokes and are defined in the previous sections. Power output is calculated using a similar expression given in Eq. (9) by substituting W_{12} and W_{34} into the equation.

VI. RESULTS

In this section, we compare UNA, STA, and STÆ Otto engines in terms of power and efficiency. To this end, we choose $\omega_c = \omega_1 = \omega_4 = 1$ and $\omega_h = \omega_2 = \omega_3 = 2.5$. We assume the durations of the two adiabatic strokes to be identical (τ_{adi}), and similarly for the two isochores (τ_{iso}). We vary τ_{adi} and τ_{iso} independently between 0.7 and 7.5. The temperatures for the cold and hot bath are taken to be $T_c = T_1 = 1$ and $T_h = T_3 = 10$, respectively. We further assume that the heat conductivities for the hot and cold isochores are equal, i.e., $\Gamma_h = \Gamma_c = 0.22$. All numerical values are given in appropriate units (energy in units of $\hbar\omega_c$, temperature in units of $\hbar\omega_c/k_B$, etc.). The parameter ranges were chosen such that

all relevant operational regimes were accessible in the analysis. Throughout this section, all the calculated efficiencies are operational except when it is directly stated otherwise. For convenience we drop the "op" superscript for the operational efficiency. We have used the open source package QuTiP for our calculations [93].

Fig. 2 compares both the power output of the three engines (top panel) and their efficiencies (bottom panel) as a function of the stroke durations, for a single cycle of operation starting from the thermal state (ω_c, T_c) which is indicated as "1" in Fig. 1. It is evident from Fig. 2(a) that for small values of τ_{adi} and τ_{iso} the UNA engine results in a negative power output and hence, does not behave as a proper heat engine. However, in STA Fig. 2(b) and STÆ Fig. 2(c) engines, a positive power output is produced even for small stroke times. It should be noted that we have not considered stroke times smaller than 0.7 because for the parameter regime that we chose, this results in trap inversion (with an infinite STA driving cost). The maximum power output of the STÆ and STA

engines occur for the smallest stroke times however for the uncontrolled engine maximum power occurs for an intermediate time $\tau_{adi} = \tau_{iso} \approx 2.3$, after which the power output declines. The figures demonstrate that the maximum power is larger for STÆ engine than the STA-only engine, which itself yields higher power than the finite-time engine with no CD-driving.

When cycle time is dominated by either isochoric or adiabatic processes the power output of the uncontrolled engine is low and, as expected, the STA engine yields higher a power output when the cycle time is dominated by the isochoric processes. However, STÆ engine outputs a relatively large values for power whether the contribution of the isochoric processes is larger for the cycle time than the adiabatic ones or vice-versa. For large values of the cycle time, the difference between the power outputs of the three engines become negligible as expected.

Fig. 2(d) shows that in the parameter regime that we have considered, the UNA engine yields a negative value for efficiency as the cycle time becomes very small. Hence, it doesn't act as a proper heat engine. Comparing Fig. 2(d), Fig. 2(e) and Fig. 2(f) we see that for small values of τ_{adi} , the efficiency is comparatively small for all three engines. However, STA and STÆ engines give larger values for the efficiency, the latter displaying a superior performance. As the cycle time becomes larger, the difference between the values of the efficiency of the three engines diminish. But it is clear that the engines with CD-driving, specifically the STÆ engine, has a larger efficiency for a bigger subset of cycle times considered for our calculations.

In order to see finer details of the performance metrics of the three engines for a subset of the cycle times considered in Fig. 2, in Fig. 3 efficiency and power of the engines are presented for $\tau_{adi} = \tau_{iso} = \tau$. In Fig. 3(a) we see a dramatic difference between the power output of the STÆ engine with the other two engines considered in this study specially for short cycle times. This figure shows a clear advantage of using CD-driving for thermalization and adiabaticity to enhance the power output. From Fig. 3(b) it is clear that for equal time allocated to isochoric and adiabatic branches, the largest to smallest efficiencies are obtained for the STÆ engine, the STA engine and the UNA engine, respectively for smaller cycle times. This demonstrates that even considering the energetic costs spent on driving the working medium to adiabaticity and thermalization, the STÆ engine is superior in terms of efficiency to both UNA and STA engines. For larger cycle times the efficiency of the three engines approach the ideal value of $1 - \omega_c/\omega_h = 0.6$. Also, for the entire of cycle times considered in this study, the efficiency of all three engines is below the Carnot efficiency $1 - T_c/T_h = 0.9$ and Curzon-Ahlborn (CA) efficiency $1 - \sqrt{T_c/T_h} \approx 0.68$. It is also worth pointing out that without considering the costs, the thermodynamic efficiency of the STÆ engine equals the ideal value throughout the considered cycle times considered in our calculations.

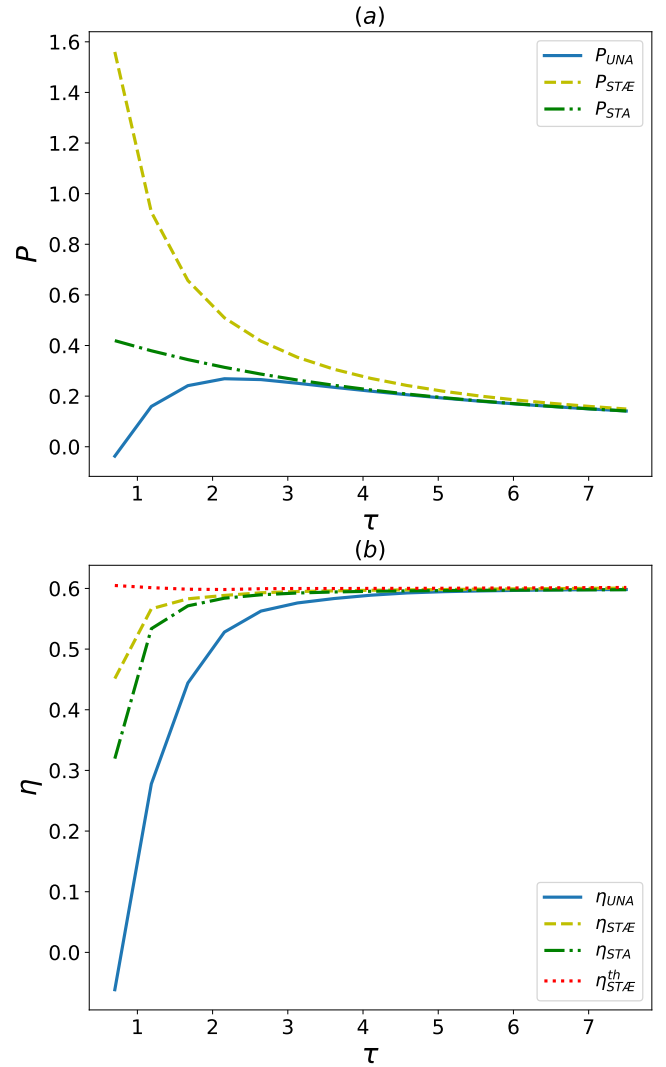


FIG. 3. Power and efficiency characteristics of the controlled and uncontrolled finite time Otto engines for an equally allocated time for their isochoric and adiabatic branches, $\tau_{iso} = \tau_{adi} = \tau$. (a) Power vs τ : UNA engine (solid blue), STA engine (green dash-dotted), STÆ engine (yellow dashed). (b) Efficiency vs τ : UNA engine (solid blue), STA engine (green dash-dotted), operational efficiency (yellow dashed) and thermodynamic efficiency (red dotted) of the STÆ engine.

In Fig. 4 we can see the control costs for the STÆ engine. As expected, Fig. 4(a) and Fig. 4(c) show that the energetic cost for CD-driving for adiabaticity decreases for longer τ_{adi} , whereas in Fig. 4(b) we can see that the cost for driving the system to thermalization shrinks as we increase τ_{iso} . This fact again verifies that the control cost given in Eq. (39) is indeed a suitable cost function for our purposes. Comparison between the maximums of the costs of the isochoric and adiabatic strokes reveal that this value is lower for thermalization than expansion, which in turn is lower than that of compression.

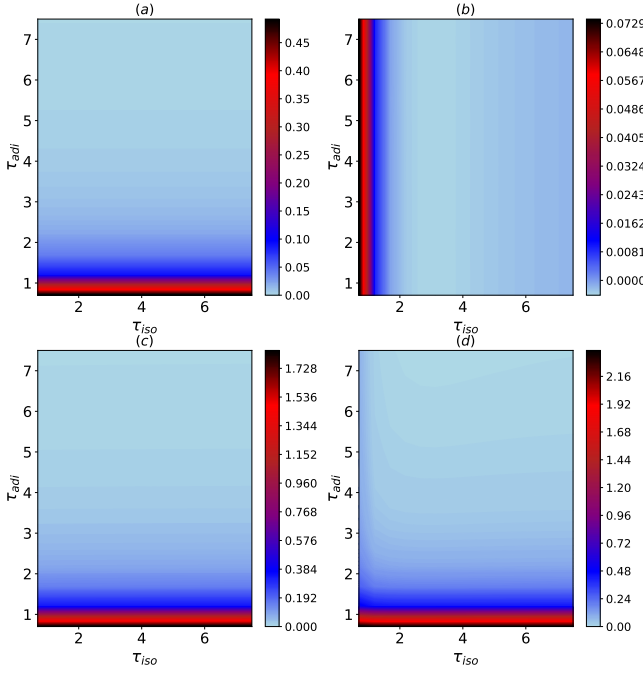


FIG. 4. Cost of the STA and STE driving for one cycle of the STA&E engine vs τ_{adi} and τ_{iso} . (a) Cost of the STA driving for adiabatic compression; (b) cost of the STE driving for hot isochore; (c) cost of the STA driving for adiabatic expansion; (d) total costs for one cycle.

Next, we move on to the performance metrics of the engines in their respective limit cycles. Our numerical calculations show that all three engines reach a limit cycle throughout the cycle times that we have considered in this study. One has to note that in the limit cycle the state of the working medium at the end of each stroke do not necessarily coincide with the ones given in the ideal Otto engine as represented by Fig. 1, unless the times allocated for each stroke are very large. Calculating the fidelity of the state of the working medium and the final state after each repetition of the cycle, we see observed that 7 cycles are enough to converge to the limit cycle of the engines for all the cycle times. In Fig. 5 the results for the power and efficiency of the engines are shown.

From Fig. 5(a) we can observe that the UNA engine yields a negative power output for a considerably large subset of allocated times for the adiabatic and isochoric strokes. Comparing Fig. 5(a) and Fig. 5(a), we see that the uncontrolled engine is much more unreliable in its limit cycle than when we only consider one cycle of operation. In comparison, Fig. 5(b) and Fig. 5(c) give a positive power output in their limit cycles for all τ_{adi} and τ_{iso} . Moreover, in Fig. 5(a) we see that in its limit cycle, the UNA engine yields a vanishingly small power outputs for cycle times dominated by isochoric/adiabatic processes. On the other hand, Fig. 5(b) shows that the

power output in the STA engine gets vanishingly small only for the cycle times dominated by adiabatic processes. However, Fig. 5(c) shows a clear advantage of using STA&E engine, in which power output is much larger compared to the UNA and STA engines, specially when we consider isochoric or adiabatic process dominated cycle times. The figure shows that similar to the case of single cycle, for the STA&E engine in its limit cycle, the power output is higher for smaller values of τ_{adi} and τ_{iso} .

The grey areas in Fig. 5(d) show that for a considerable section of the considered allocated times for the isochoric and adiabatic strokes, the uncontrolled engine doesn't act as a proper heat engine. In its limit cycle the efficiency of the UNA engine is low compared to the STA&E and the STA engines except when τ_{iso} and τ_{adi} are both large. In this case the expansion and compression strokes approach their adiabatic evolution and in the end of the isochoric strokes the fidelity between the density matrix of working medium and the ideal thermal state of for the temperature of the respective bath is almost unity. Comparing Fig. 5(e) and Fig. 5(f) we see that surprisingly, for cycles with small τ_{iso} , the efficiency of the STA&E engine is smaller than that of the STA engine except when τ_{adi} is also small. Although, this doesn't mean that the STA-only engine is superior to the STA&E engine for the mentioned cycle time allocations because in this case, as seen in Fig. 5(b) the power output of the STA-only engine becomes much smaller than the STA&E engine. We can also clearly see that the maximum value attained for efficiency is larger for the STA&E engine than the STA engine when we consider the entirety of the parameter regime. An interesting aspect of the STA&E protocol limit cycles is that the performance is non-monotonous in τ_{adi} . As a result, high-power/high-efficiency islands appear, such as the one observed around $\tau_{adi} = \tau_{iso} \approx 1.6$ in Fig. 5(f).

In order to make a more detailed the comparison of the performance metrics of the engines for a subset of the stroke times considered in this study, in Fig. 6 we present efficiency and power of the heat engines for $\tau_{adi} = \tau_{iso} = \tau$. In Fig. 6(a) we can see that the STA&E engine yields a much higher power output than the STA and UNA engines. Comparing Fig. 3(a) and Fig. 6(a) we see that in their limit cycle, the power of the STA and UNA engines get reduced, as compared with the case of single cycle, throughout the cycle times. However, for the STA&E engine the power output for the limit cycle is higher than that of the single cycle for the entirety of the cycle time.

As shown in Fig. 6(b), in its limit cycle, the efficiency of the STA&E engine is no longer monotonic in the cycle time. The difference between the efficiencies of the uncontrolled engine and the controlled engines is more dramatic in their limit cycles and their efficiency values don't approach each other to the ideal value of $1 - \omega_c/\omega_h = 0.6$ unless the cycle time is very large. The results show that

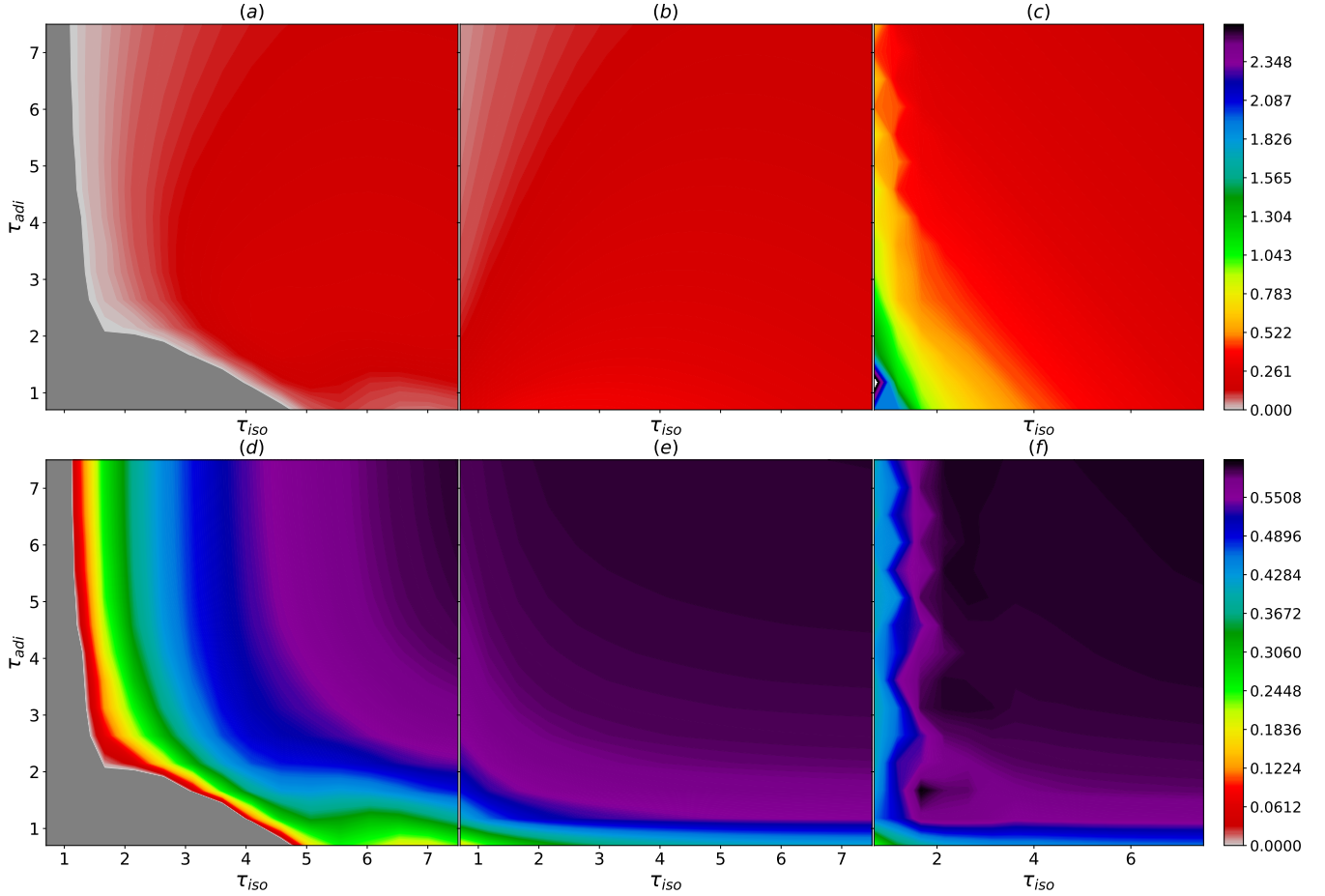


FIG. 5. Power and efficiency of the Otto engine at its limit cycle as a function of the duration of the isochoric and adiabatic branches. Top row: Limit cycle power vs τ_{adi} and τ_{iso} for the (a) UNA engine; (b) STA engine; (c) STÆ engine. Bottom row: Limit cycle efficiency vs τ_{adi} and τ_{iso} for the (d) UNA engine; (e) STA engine; (f) STÆ engine. Negative power and efficiency results for the finite time Otto engine are greyed out.

the STÆ engine has higher efficiency than the STA engine, specially for smaller cycle times.

In Fig. 7 the costs for CD-driving at the limit cycle for the STÆ engine are presented. Similar to the case of single cycle, we can see that the cost of the hot isochoric and adiabatic strokes are highest for short τ_{iso} and τ_{adi} respectively. However, for short cycle times in the limit cycle the share of the thermalization cost is the highest in the total control cost as opposed to the case of single cycle. Again, as τ_{adi} and τ_{iso} is increased, the control costs of the adiabatic and hot isochoric strokes decreases. However, for small τ_{adi} in the limit cycle, the cost for CD-driving during the expansion and compression strokes becomes relatively small for larger τ_{iso} as opposed to what we see for a single cycle.

VII. CONCLUSION

In conclusion, we studied the thermodynamic performance of a quantum harmonic Otto engine in finite

time and compared three cases of Otto engine with no CD-driving, Otto engine with STA on the adiabatic strokes and Otto engine with STA on the hot isochoric branch. We have included the costs of driving the engine for calculating the thermodynamic figures of merit. In our calculations we have considered two modes of operation. First we studied the thermodynamic performance criteria for a single cycle and then we calculated the same figures of merit for the engines running in their respective limit cycles.

Our results for single cycle indicate that controlling the hot thermalization process in the Otto engine greatly increases the power output of the engine specifically for short cycle time durations. Also, even taking the control costs into account, the STÆ engine yields a higher efficiency than the STA and UNA engines. For a single cycle starting from the thermal state of the cold bath, the control costs for thermalization is lower than that of the compression and expansion strokes.

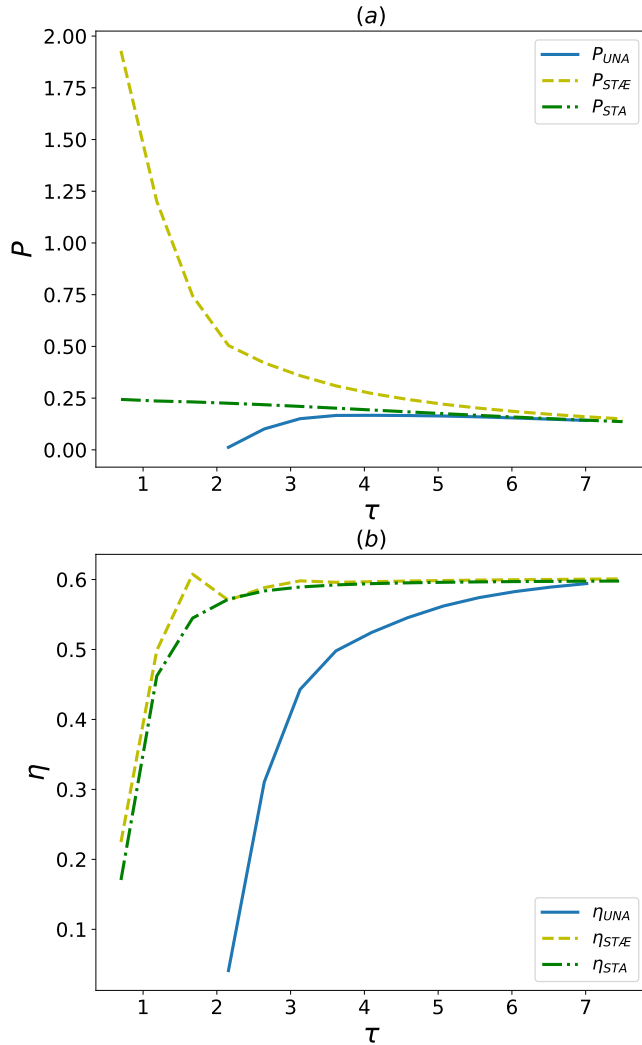


FIG. 6. Limit cycle power and efficiency characteristics of the controlled and uncontrolled finite time Otto engines for an equally allocated time for their isochoric and adiabatic branches, $\tau_{iso} = \tau_{adi} = \tau$. (a) Limit cycle power vs τ : UNA engine (solid blue), STA engine (green dash-dotted), STÆ engine (yellow dashed) of the engine with STA on its adiabatic strokes and STE on its hot isochore. (b) Limit cycle efficiency vs τ : UNA engine (solid blue), STA engine (green dash-dotted), STÆ engine (yellow dashed). Negative power and efficiency results for the finite time Otto engine are not displayed.

In total, the control costs decline as we increase the time allocated for the isochoric and adiabatic branches. Our calculations show that for the UNA engine the parameter regime of the stroke time durations for which the power output and efficiency are negative greatly increases in its limit cycle as compared to only

a single cycle of operation. For the CD-driven engines (both STA and STÆ), the power output remains positive throughout the stroke times considered in this study.

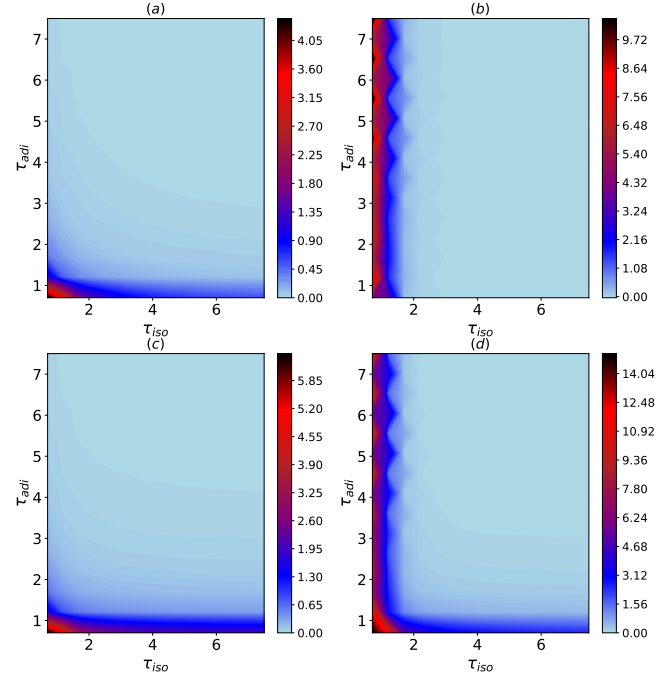


FIG. 7. Cost of the STA and STE driving for the limit cycle of the STÆ engine vs τ_{adi} and τ_{iso} . (a) Cost of the STA driving for adiabatic compression; (b) cost of the STE driving for hot isochore; (c) cost of the STA driving for adiabatic expansion; (d) total costs for one cycle.

Our numerical calculations show that in the limit cycle, the efficiency vs cycle time is not necessarily monotonic for cycle time for the STÆ engine, and the power for this engine in this mode of operation increases unlike the STA and UNA engines compared to the single cycle case. In its limit cycle, the thermalization cost dominates the control costs for the STÆ engine, especially for small time allocation for the isochoric branches. However, similar to the single cycle case, the costs decline as the cycle time is increased. In addition to illuminating the fundamental potential and energetic cost limitations of finite-time quantum heat engines with shortcuts to adiabaticity and equilibration, our results can be significant for their practical implementations with optimum power and efficiency.

ACKNOWLEDGMENTS

We gratefully acknowledge M. T. Naseem, B. Çakmak, and O. Pusuluk for fruitful discussions.

- [1] S. Carnot, R. H. Thurston, R. H. Carnot, and B. Kelvin, William Thomson, *Reflections on the motive power of heat and on machines fitted to develop that power* (New York :J. Wiley,) p. 292, <https://www.biodiversitylibrary.org/bibliography/17778>.
- [2] F. L. Curzon and B. Ahlborn, American Journal of Physics **43**, 22 (1975), <https://doi.org/10.1119/1.10023>.
- [3] R. Kosloff and A. Levy, Annual Review of Physical Chemistry **65**, 365 (2014), pMID: 24689798, <https://doi.org/10.1146/annurev-physchem-040513-103724>.
- [4] R. Kosloff and Y. Rezek, Entropy **19**, 136 (2017).
- [5] A. Tuncer and O. E. Müstecaplıoğlu, Turkish Journal of Physics **44**, 404 (2020).
- [6] G. Kurizki and A. G. Kofman, *Thermodynamics and Control of Open Quantum Systems* (Cambridge University Press, 2022).
- [7] S. Deffner and S. Campbell, *Quantum Thermodynamics*, 2053-2571 (Morgan & Claypool Publishers, 2019).
- [8] H. E. D. Scovil and E. O. Schulz-DuBois, Phys. Rev. Lett. **2**, 262 (1959).
- [9] R. Alicki, **12**, L103 (1979).
- [10] R. Kosloff, The Journal of Chemical Physics **80**, 1625 (1984), <https://doi.org/10.1063/1.446862>.
- [11] E. Geva and R. Kosloff, The Journal of Chemical Physics **96**, 3054 (1992), <https://doi.org/10.1063/1.461951>.
- [12] E. Geva and R. Kosloff, The Journal of Chemical Physics **104**, 7681 (1996), https://pubs.aip.org/aip/jcp/article-pdf/104/19/7681/10779587/7681_1_online.pdf.
- [13] T. Feldmann, E. Geva, R. Kosloff, and P. Salamon, American Journal of Physics **64**, 485 (1996), https://pubs.aip.org/aapt/ajp/article-pdf/64/4/485/12120289/485_1_online.pdf.
- [14] M. O. Scully, Phys. Rev. Lett. **88**, 050602 (2002).
- [15] T. E. Humphrey, R. Newbury, R. P. Taylor, and H. Linke, Phys. Rev. Lett. **89**, 116801 (2002).
- [16] M. O. Scully, M. S. Zubairy, G. S. Agarwal, and H. Walther, Science **299**, 862 (2003).
- [17] T. Feldmann and R. Kosloff, Phys. Rev. E **68**, 016101 (2003).
- [18] T. D. Kieu, Phys. Rev. Lett. **93**, 140403 (2004).
- [19] T. Feldmann and R. Kosloff, Phys. Rev. E **70**, 046110 (2004).
- [20] H. T. Quan, P. Zhang, and C. P. Sun, Phys. Rev. E **72**, 056110 (2005).
- [21] Y. Rezek and R. Kosloff, New Journal of Physics **8**, 83 (2006).
- [22] H. T. Quan, Y.-x. Liu, C. P. Sun, and F. Nori, Phys. Rev. E **76**, 031105 (2007).
- [23] A. E. Allahverdyan, R. S. Johal, and G. Mahler, Phys. Rev. E **77**, 041118 (2008).
- [24] O. Abah, J. Roßnagel, G. Jacob, S. Deffner, F. Schmidt-Kaler, K. Singer, and E. Lutz, Phys. Rev. Lett. **109**, 203006 (2012).
- [25] D. Gelbwaser-Klimovsky and G. Kurizki, Phys. Rev. E **90**, 022102 (2014).
- [26] A. Ü. C. Hardal and Ö. E. Müstecaplıoğlu, Scientific Reports **5**, 12953 (2015).
- [27] D. Newman, F. Mintert, and A. Nazir, Phys. Rev. E **95**, 032139 (2017).
- [28] D. Turkpence, F. Altintas, M. Paternostro, and Özgür E. Müstecaplıoğlu, Europhysics Letters **117**, 50002 (2017).
- [29] B. K. Agarwalla, J.-H. Jiang, and D. Segal, Phys. Rev. B **96**, 104304 (2017).
- [30] A. U. C. Hardal, N. Aslan, C. M. Wilson, and O. E. Müstecaplıoğlu, Phys. Rev. E **96**, 062120 (2017).
- [31] W. Niedenzu, V. Mukherjee, A. Ghosh, A. G. Kofman, and G. Kurizki, Nature Communications **9**, 165 (2018).
- [32] A. Insinga, B. Andresen, P. Salamon, and R. Kosloff, Phys. Rev. E **97**, 062153 (2018).
- [33] M. T. Naseem and Özgür E. Müstecaplıoğlu, J. Opt. Soc. Am. B **36**, 3000 (2019).
- [34] E. Köse, S. Çakmak, A. Gençten, I. K. Kominis, and O. E. Müstecaplıoğlu, Phys. Rev. E **100**, 012109 (2019).
- [35] V. Singh and O. E. Müstecaplıoğlu, Phys. Rev. E **102**, 062123 (2020).
- [36] S. H. Raja, S. Maniscalco, G. S. Paraoanu, J. P. Pekola, and N. L. Gullo, New Journal of Physics **23**, 033034 (2021).
- [37] Y. Zou, Y. Jiang, Y. Mei, X. Guo, and S. Du, Phys. Rev. Lett. **119**, 050602 (2017).
- [38] J. Klatzow, J. N. Becker, P. M. Ledingham, C. Weinzel, K. T. Kaczmarek, D. J. Saunders, J. Nunn, I. A. Walmsley, R. Uzdin, and E. Poem, Phys. Rev. Lett. **122**, 110601 (2019).
- [39] J. P. S. Peterson, T. B. Batalhão, M. Herrera, A. M. Souza, R. S. Sarthour, I. S. Oliveira, and R. M. Serra, Phys. Rev. Lett. **123**, 240601 (2019).
- [40] Q. Bouton, J. Nettersheim, S. Burgardt, D. Adam, E. Lutz, and A. Widera, Nature Communications **12**, 2063 (2021).
- [41] J. Sheng, C. Yang, and H. Wu, Science Advances **7**, eabl7740 (2021), <https://www.science.org/doi/pdf/10.1126/sciadv.abl7740>.
- [42] V. F. Lisboa, P. R. Dieguez, J. R. Guimarães, J. F. G. Santos, and R. M. Serra, Phys. Rev. A **106**, 022436 (2022).
- [43] J.-W. Zhang, J.-Q. Zhang, G.-Y. Ding, J.-C. Li, J.-T. Bu, B. Wang, L.-L. Yan, S.-L. Su, L. Chen, F. Nori, S. K. Özdemir, F. Zhou, H. Jing, and M. Feng, Nature Communications **13**, 6225 (2022).
- [44] I. Reyes-Ayala, M. Miotti, M. Hemmerling, R. Dubessy, H. Perrin, V. Romero-Rochin, and V. S. Bagnato, Entropy **25**, 10.3390/e25020311 (2023).
- [45] J. Roßnagel, O. Abah, F. Schmidt-Kaler, K. Singer, and E. Lutz, Phys. Rev. Lett. **112**, 030602 (2014).
- [46] M. Campisi and R. Fazio, Nature Communications **7**, 11895 (2016).
- [47] M. Kim, M. Scully, and A. Svidzinsky, Nature Photonics **16**, 669 (2022).
- [48] E. Torrontegui, S. Ibáñez, S. Martínez-Garaot, M. Modugno, A. del Campo, D. Guéry-Odelin, A. Ruschhaupt, X. Chen, and J. G. Muga, in *Advances in Atomic, Molecular, and Optical Physics*, Advances In Atomic, Molecular, and Optical Physics, Vol. 62, edited by E. Arimondo, P. R. Berman, and C. C. Lin (Academic Press, 2013) pp. 117–169.
- [49] D. Guéry-Odelin, A. Ruschhaupt, A. Kiely, E. Torrontegui, S. Martínez-Garaot, and J. G. Muga, Rev. Mod. Phys. **91**, 045001 (2019).

- [50] M. Demirplak and S. A. Rice, *The Journal of Physical Chemistry A* **107**, 9937 (2003), <https://doi.org/10.1021/jp030708a>.
- [51] M. Demirplak and S. A. Rice, *The Journal of Physical Chemistry B* **109**, 6838 (2005), pMID: 16851769, <https://doi.org/10.1021/jp040647w>.
- [52] M. V. Berry, *Journal of Physics A: Mathematical and Theoretical* **42**, 365303 (2009).
- [53] X. Chen, A. Ruschhaupt, S. Schmidt, A. del Campo, D. Guéry-Odelin, and J. G. Muga, *Phys. Rev. Lett.* **104**, 063002 (2010).
- [54] X. Chen, E. Torrontegui, and J. G. Muga, *Phys. Rev. A* **83**, 062116 (2011).
- [55] A. del Campo, *Phys. Rev. A* **84**, 031606 (2011).
- [56] A. d. Campo and M. G. Boshier, *Scientific Reports* **2**, 648 (2012).
- [57] S. Masuda and K. Nakamura, *Proceedings of the Royal Society A: Mathematical, Physical and Engineering Sciences* **466**, 1135 (2010), <https://royalsocietypublishing.org/doi/pdf/10.1098/rspa.2009.0446>.
- [58] S. Masuda and K. Nakamura, *Phys. Rev. A* **84**, 043434 (2011).
- [59] E. Torrontegui, S. Martínez-Garaot, A. Ruschhaupt, and J. G. Muga, *Phys. Rev. A* **86**, 013601 (2012).
- [60] A. Vepsäläinen, S. Danilin, and G. S. Paraoanu, *Science Advances* **5**, eaau5999 (2019), <https://www.science.org/doi/pdf/10.1126/sciadv.aau5999>.
- [61] A. Vepsäläinen and G. S. Paraoanu, *Advanced Quantum Technologies* **3**, 1900121 (2020), <https://onlinelibrary.wiley.com/doi/pdf/10.1002/qute.201900121>.
- [62] H. Zhou, Y. Ji, X. Nie, X. Yang, X. Chen, J. Bian, and X. Peng, *Phys. Rev. Appl.* **13**, 044059 (2020).
- [63] Z. Yin, C. Li, J. Allcock, Y. Zheng, X. Gu, M. Dai, S. Zhang, and S. An, *Nature Communications* **13**, 188 (2022).
- [64] K. Funo, N. Lambert, B. Karimi, J. P. Pekola, Y. Matsuyama, and F. Nori, *Phys. Rev. B* **100**, 035407 (2019).
- [65] O. Abah, M. Paternostro, and E. Lutz, *Phys. Rev. Res.* **2**, 023120 (2020).
- [66] A. d. Campo, J. Goold, and M. Paternostro, *Scientific Reports* **4**, 6208 (2014).
- [67] O. Abah and E. Lutz, *Phys. Rev. E* **98**, 032121 (2018).
- [68] O. Abah and M. Paternostro, *Phys. Rev. E* **99**, 022110 (2019).
- [69] M. Beau, J. Jaramillo, and A. Del Campo, *Entropy* **18**, 10.3390/e18050168 (2016).
- [70] B. Çakmak and O. E. Müstecaplıoğlu, *Phys. Rev. E* **99**, 032108 (2019).
- [71] A. Hartmann, V. Mukherjee, W. Niedenzu, and W. Lechner, *Phys. Rev. Res.* **2**, 023145 (2020).
- [72] B. Çakmak, *Turkish Journal of Physics* **45**, 59 (2021).
- [73] R. Dann, A. Levy, and R. Kosloff, *Phys. Rev. A* **98**, 052129 (2018).
- [74] R. Dann, A. Tosalina, and R. Kosloff, *Phys. Rev. Lett.* **122**, 250402 (2019).
- [75] T. Villazon, A. Polkovnikov, and A. Chandran, *Phys. Rev. A* **100**, 012126 (2019).
- [76] S. Alipour, A. Chenu, A. T. Rezakhani, and A. del Campo, *Quantum* **4**, 336 (2020).
- [77] L. Dupays, I. L. Egusquiza, A. del Campo, and A. Chenu, *Phys. Rev. Research* **2**, 033178 (2020).
- [78] N. Pancotti, M. Scandi, M. T. Mitchison, and M. Perarnau-Llobet, *Phys. Rev. X* **10**, 031015 (2020).
- [79] N. Suri, F. C. Binder, B. Muralidharan, and S. Vinjanampathy, *The European Physical Journal Special Topics* **227**, 203 (2018).
- [80] R. Dann and R. Kosloff, *New Journal of Physics* **22**, 013055 (2020).
- [81] S. Alipour, A. T. Rezakhani, A. Chenu, A. del Campo, and T. Ala-Nissila, *Phys. Rev. A* **105**, L040201 (2022).
- [82] S. Deffner and E. Lutz, *Phys. Rev. E* **77**, 021128 (2008).
- [83] S. Deffner, O. Abah, and E. Lutz, *Chemical Physics* **375**, 200 (2010), stochastic processes in Physics and Chemistry (in honor of Peter Hänggi).
- [84] V. Singh, S. Singh, O. Abah, and O. E. Müstecaplıoğlu, *Phys. Rev. E* **106**, 024137 (2022).
- [85] J. Watrous, *Unital channels and majorization*, in *The Theory of Quantum Information* (Cambridge University Press, 2018) p. 201–249.
- [86] G. Lindblad, *Communications in Mathematical Physics* **40**, 147 (1975).
- [87] D. Petz, *Linear Algebra and its Applications* **244**, 81 (2009).0446996.
- [88] A. Frigerio, *Letters in Mathematical Physics* **2**, 79 (1977).
- [89] S. Deffner, C. Jarzynski, and A. del Campo, *Phys. Rev. X* **4**, 021013 (2014).
- [90] J. G. Muga, X. Chen, S. Ibáñez, I. Lizuain, and A. Ruschhaupt, *Journal of Physics B: Atomic, Molecular and Optical Physics* **43**, 085509 (2010).
- [91] H. Mishima and Y. Izumida, *Phys. Rev. E* **96**, 012133 (2017).
- [92] H. Spohn, *Journal of Mathematical Physics* **19**, 1227 (2008), https://pubs.aip.org/aip/jmp/article-pdf/19/5/1227/11195978/1227_1_online.pdf.
- [93] J. R. Johansson, P. D. Nation, and F. Nori, *Computer Physics Communications* **183**, 1760 (2012).
- [94] R. Kosloff and T. Feldmann, *Phys. Rev. E* **65**, 055102 (2002).
- [95] A. Frigerio, *Communications in Mathematical Physics* **63**, 269 (1978).